Short Communication

A Quantum Chemical Study on Some Schiff Bases as Inhibitors of Mild Steel Corrosion in HCl Solution

Shuangkou Chen[*], *Yuting Ren, Bei Luo, Yinying Guo, Ying Peng*

College of Chemistry and Chem-engineering, Chongqing University of Science and Technology, Chongqing 401331, China
[*]E-mail: cskcn@yeah.net

A quantum chemical study using a DFT/6-31+G(d) method has been performed on three types of Schiff base compound that are used as corrosion inhibitors for mild steel to determine the relationship between their molecular structures and their inhibition efficiency(*IE*). HOMO orbital (E_{HOMO}) and LUMO orbital (E_{LUMO}) energies and other physical properties have been calculated, with these results showing that *IE* had a good linear relationship to ΔE, η, σ and Q_N charge (imino nitrogen). These theoretical results were in accord with previously reported experimental results and have been used to identify some new homologous Schiff base compounds that are predicted to exhibit better corrosion inhibition performance.
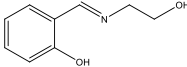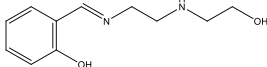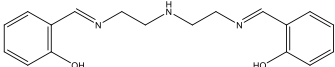
1. INTRODUCTION

Malleable mild steel is cheap and easy to prepare and widely used by the petroleum industry, with HCl often used in oil and gas fields to clean its metal surfaces and remove rust, with organic compounds/polymers often used as coatings to inhibit corrosion of its metal surface[1-1]. Some of these inhibitors contain functional groups[3-6] that can donate electrons to the metal surface, with Schiff base inhibitors having previously been reported as corrosion inhibitors for mild steel in acidic solution[7-14]. Küstü et al. have previously used weight loss, polarization and impedance techniques to study the inhibitory effects of three kinds of Schiff base compounds on the corrosion behavior of mild steel in 2M HCl solution at 298K (Table 1) 15. Quantum chemical methods combined with experimental results have previously been used to investigate the structure and performance of corrosion inhibitors[16-18]. This theoretical study has carried out an investigation to correlate quantum chemical parameters of these Schiff base compounds with their experimentally determined corrosion efficiencies. The following structural parameters of these compounds were calculated: HOMO orbital

energy(E_{HOMO}), LUMO orbital energy(E_{LUMO}), energy gap (ΔE), some charge distributions (Q), dipole movement (μ) , the absolute electro-negativity values (χ), global hardness (η), electron affinity (A), softness (σ), ionization potential (I) and the fraction of electrons transferred (ΔN). Linear regression analysis methods have been used to determine which parameters are most important for corrosion inhibition efficiency *IE,* with the results of this study being used to identify the structures of new imine analogues that are predicted to exhibit enhanced corrosion inhibition properties.

Table 1. Abbreviations and molecular structures of the studied compounds.

Inhibitors	Conformation	Abbreviation
2-{(E)-[(2-hydroxyethyl)imino]methyl}phenol		M1
2-[(E)-({2-[(2-hydroxyethyl)amino] ethyl} imino)methyl] phenol		M2
2,2'-{iminobis[ethane-2,1-diylnitrilo(E)methylylidene]} diphenol		M3

2. THEORY AND COMPUTATIONAL DETAILS

DFT (density functional theory) methods**Error! Reference source not found.**-23] were used to optimize structures and quantum parameters for the three classes of Schiff base compound, using a 6-31+G(d) basis set with B3LYP functional to carry out calculations [24-25]. HOMO (E_{HOMO}) and LUMO (E_{LUMO}) orbital energies for these imines were optimized and verified without imaginative frequencies. The effect of solvent was determined employing an SMD model using a dielectric constant of 78.5 for water26, with all calculations performed using Gaussian09 software26.

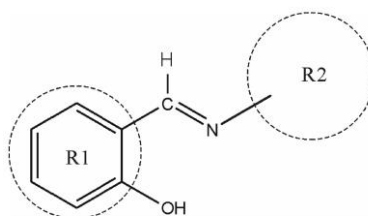## 3. RESULTS AND DISCUSSION

Figure 1. The molecular structure of inhibitor

Figure 1 shows the molecular structure of the corrosion inhibitors investigated in this study, with Table 2 containing their structural parameters that were determined using quantum chemical calculations. E_{HOMO} and E_{LUMO} are defined as the energies of the HOMO and LUMO orbitals of each inhibitor, respectively, whilst ΔE ($\Delta E = E_{HOMO} - E_{LUMO}$) is the energy gap between them. According to

Koopman's theorem28，the ionization potential (*I*) and electron affinity (*A*) values of a compound are related to the energies of its HOMO and LUMO orbitals, where: $I=-E_{HOMO}$ and $A=-E_{LUMO}$. Absolute electronegativity (χ) and global hardness (η)29 values were calculated using the equations: $\chi=(I+A)/2$ and $\eta=(I-A)/2$, respectively, with softness values defined using the equation : $\sigma=1/\eta$. These values could be used to calculate the fraction of electron density transferred from the inhibitor to the iron surface [30-31], which has the following format: $N=(\chi_{Fe}-\chi_{inh})/2(\eta_{Fe}+\eta_{inh})$, where, χ_{Fe}=7.0 eV/mol and η_{Fe}=0 eV/mol for iron and $I=A$ 29. Q_{R1} refers to a carbon atom's net charge when present in a benzene ring (R1); Q_{-OH} refers to the net charge of an -OH group; Q_N and Q_C refer to the net charges of the N and C atoms of a -CH=N- group; $Q_{N=C}$ refers to the total charge of N and C of a -CH=N- group; Q_{R2} refers to the total charge of an R2 group.

Table 2. Quantum chemical parameters for inhibitors calculated at B3LYP/6-31+G (d) level.

Inhibitor	E_{HOMO} (eV)	E_{LUMO} (eV)	ΔE (eV)	μ (debye)	η (eV)	x eV	σ eV^{-1}	ΔN	Q_{R1}	Q_{-OH}	Q_N	Q_C	$Q_{N=C}$	Q_{R2}	$IE\%^a$
M1	-6.361	-1.428	4.933	4.435	2.466	3.895	0.405	0.630	-0.535	-0.172	-0.232	-0.294	-0.526	-0.183	67.0
M2	-6.202	-1.395	4.807	5.248	2.404	3.798	0.416	0.666	-0.542	-0.173	-0.221	-0.373	-0.594	-0.175	79.0
M3	-6.141	-1.503	4.638	4.745	2.319	3.822	0.431	0.685	-0.522	-0.173	-0.204	-0.420	-0.624	-0.195	93.0

[a] Exp. value from Ref. 15, the inhibition efficiency (*IE*) for the corrosion of mild steel tested using weight loss measurements in 2M HCl solution with addition of 10^{-2} mol/L of various inhibitors.

Unitary or linear calculations that correlate corrosion *IE* to quantum chemical parameters were used to establish regression equations, multiple correlation coefficients (R and R^2). These values (with R^2 coefficients close to 0.99) were then used to determine correlation coefficients for formula (3), (4), (6) and (8) (see Table 3).

Table 3. The regression equations of corrosion inhibition efficiency and their structural parameters

Variable	Regression equation	Formula	Multiple R	R^2
E_{HOMO}	$IE=762.316+109.496\times E_{HOMO}$	(1)	0.95703	0.9159
E_{LUMO}	$IE=-160.926-166.866\times E_{LUMO}$	(2)	0.70762	0.5007
E_{HOMO}, E_{LUMO}	$IE=539.620+91.718\times E_{HOMO} - 77.581\times E_{LUMO}$	(3)	0.99970	0.9994
ΔE	$IE= 500.653-87.840\times\Delta E$	(4)	0.99918	0.9984
μ	$IE=28.343+10.671\times\mu$	(5)	0.33645	0.1132
η	$IE=500.653-175.681\times\eta$	(6)	0.99918	0.9984
x	$IE=773.277-180.715\times x$	(7)	0.69619	0.4847
σ	$IE=-338.885+1002.338\times\sigma$	(8)	0.99833	0.9967
ΔN	$IE=-216.462+448.477\times\Delta N$	(9)	0.97592	0.9524
Q_{R1}	$IE=540.220+864.078\times Q_{R1}$	(10)	0.67391	0.4542
Q_{-OH}	$IE=-3201.000-19000.000\times Q_{-OH}$	(11)	0.84299	0.7106
Q_N	$IE=281.059+919.598\times Q_N$	(12)	0.99690	0.9938
Q_C	$IE=6.950-200.691\times Q_C$	(13)	0.98201	0.9643
$Q_{N=C}$	$IE=-65.743-250.132\times Q_{N=C}$	(14)	0.96519	0.9316
Q_{R2}	$IE=-70.710-815.789\times Q_{R2}$	(15)	0.63108	0.3983

3.1 Correlation between molecular orbital energies and IE

Inhibitor adsorption processes were studied using frontier molecular orbital theory32, with the HOMO and LUMO frontier orbitals of the three inhibitors shown in Figure 2 showing similar activity coefficients. The HOMO orbitals are largely located on R1 (benzene ring) and the -CH=N- groups. The HOMO orbital distribution of these inhibitors was relatively uniform, which enables the imine to adsorb strongly to the metal surface, resulting in electron density from the HOMO orbital of the inhibitor being transferred to the empty orbitals of the metal surface. Table 3 shows that the higher the energy of the HOMO orbital, the better its performance as an inhibitor, with the M3 imine exhibiting the highest HOMO energy (-6.141eV) and the best corrosion inhibition performance of 93.0%.

The HOMO-LUMO energy gap (ΔE) is another important factor affecting the performance of corrosion inhibitors, with a low (ΔE) favoring electron transfer to the empty orbitals of the metal surface. This means that *IE* values increase as ΔE values decrease, with the relationship between *IE* and ΔE given the formula: $IE= 500.653-87.840\times\Delta E$, with a good $R^2=0.99918$ value observed for this correlation.
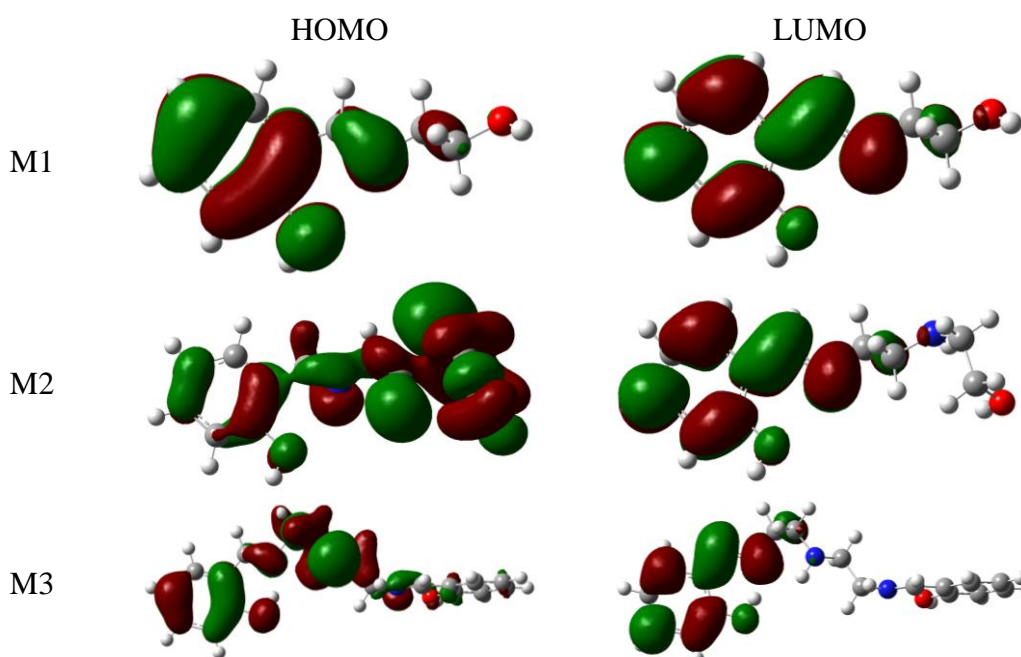

Figure 2. Frontier molecule orbitals of the three Schiff base inhibitors

Other molecular parameters, such as dipole moment (μ), absolute electronegativity values (χ), electron affinities (A), global hardness (η), global softness (σ), ionization potentials (I) and the fraction of electrons transferred from inhibitors to iron (ΔN) were also calculated (Table 2). The multi-linear regression function relationships between these parameters and corrosion *IE* are shown in Table 3, which reveals that *IE* has a good relationship with global hardness (η), softness (σ) and ΔN. The correlation coefficients of these equations (formula (6), (8) and (9)) were in the range 0.97~0.99, indicating that they affect the performance of corrosion inhibitors significantly.

Global hardness and softness can determine the stability and reactivity of corrosion inhibitors,

with hard inhibitors often exhibiting large HOMO-LUMO energy gaps, whilst soft inhibitors normally have a small HOMO-LUMO energy gap. Therefore, soft corrosion inhibitors often have better activities than hard inhibitors, because they can more easily donate electrons to the metal surface 33. In this study, the M3 imine was shown to exhibit the lowest hardness value (2.319eV) and highest softness value ($0.431eV^{-1}$), which correlated with it exhibiting the best corrosion inhibition performance.

ΔN is another important factor affecting corrosion inhibition performance, with higher *ΔN* values (more electrons transferred from inhibitor to iron surface) corresponding to increased *IE* values[28, 30]. The Schiff base inhibitors used in this study form an absorption layer that donates electrons to the iron surface, which serves to help prevent surface corrosion. Inhibitor M3 gave the highest *IE* value, because it has the highest HOMO energy (E_{HOMO}= -6.141eV) and *ΔN* (*ΔN=0.685*) values, that result in greater numbers of electrons being transferred to the metal surface .

3.2 Correlation between Mulliken charge and inhibition efficiency

The relationship between the Mulliken charge of various atoms (or groups) and experimentally determined *IE* values were also determined, using linear regression to analyze the net charges - Q_{R1}, Q_{OH}, Q_N, Q_C, $Q_{N=C}$ and Q_{R2}. The Mulliken charges for nitrogen and carbon atoms were found to be well correlated, affording R values of 0.9960 and 0.982, respectively, whilst the charges of the N=C group gave an R value of 0.965. This indicates that the contributions of the N and C atoms and the N=C group to *IE* are much greater than the contributions from the R1, R2 and -OH groups. This indicates that donation of electron density from the lone pair of the N=C group to the metal plays a major role in determining the corrosion performance of these Schiff base inhibitors.

To further investigate which part of the inhibitor plays a critical role for corrosion inhibition, molecular electrostatic surface potentials were determined using DFT/6-31+G(d) calculations, which showed that the majority of negative charge was centered on the heteroatoms of the N=C and -OH groups (see Figure 3). Therefore, it is likely that adsorption of these inhibitors to the metal surface occurs through their N=C and -OH groups, which explains why the Q_N, Q_C and $Q_{N=C}$ and Q_{OH} charge values correlate best with their overall *IE* levels.

          M1   M2   M3
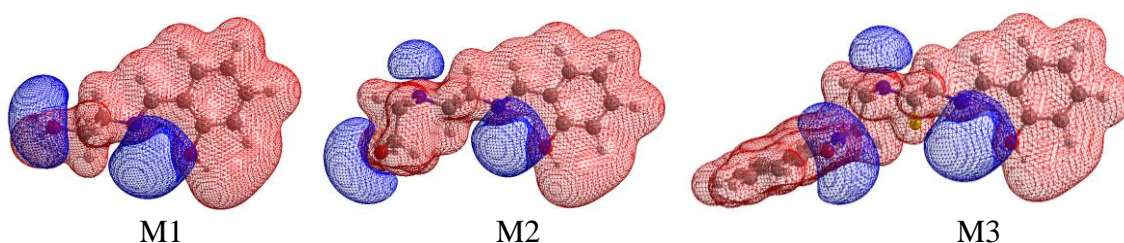**Figure 3.** The molecular electrostatic potential surface of three inhibitors
* Blue: negative, Red: positive

3.3 Interaction between inhibitors & Fe(100) surface and corrosion-inhibition mechanism

As these Schiff bases compounds used as inhibitors of mild steel corrosion in HCl solution, a two layers Fe(100) surface constructed by cluster of $Fe_{53}(32,21)$ was selected for molecular mechanics simulation in order to study the interaction and corrosion-inhibition mechanism. During the simulation, we find that regardless of the initial state of these molecules, the inhibitors always tend to adsorb parallel to the metal surface. In addition, we also calculated the electrostatic potential surfaces (Figrure 4). From Figure 4 we can find that after the adsorption, there are some electrons transferred from inhibitor to Fe(100)surface. The surface in Fig. 4(a) received the least electrons($\Delta N=0.630$) and that in Fig. 4(c) receives the most ($\Delta N=0.685$). This also explains intuitively why M3 has the best inhibition performance.
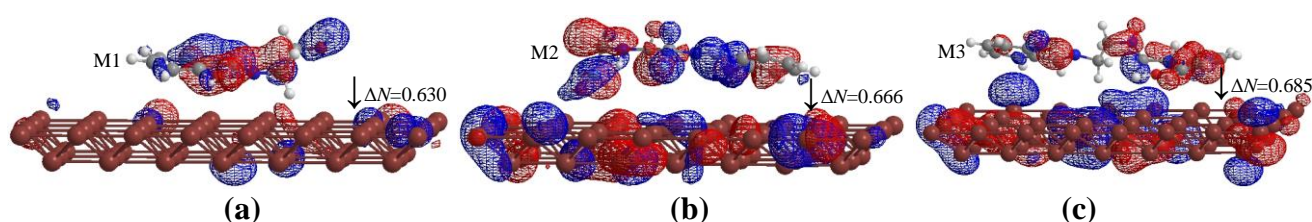

Figure 4. Adsorption configuration and the charge distribution surfaces for inhibitors on Fe(100)
  * Blue: negative, Red: positive

On the basis of the interaction studies, the adsorption behavior of these corrosion inhibitors on the metal surface may be mainly chemical adsorption because of the apparent electrons transferred during this process. The adsorption and corrosion inhibition mechanism in HCl solution could be explained as follows:

$Fe \rightarrow Fe^{2+}+2e$

$[M] \rightarrow [M]^{\Delta N+}+\Delta Ne$

$\Delta Ne+(\Delta N/2)Fe^{2+} \rightarrow Fe$
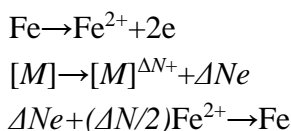
In HCl solution, Fe has the tendency to lose electrons to become iron ions and corrosion inhibitor molecules could provide electrons to the metal to become corrosion inhibitor cations; then the inhibitor cations are adsorbed on the metal surface, preventing the same positively charged hydrogen ions from contacting metal surfaces in the solution (Figure 5). Therefore, these compounds acts as a corrosion inhibitor and the metal surface has been protected from corrosion.
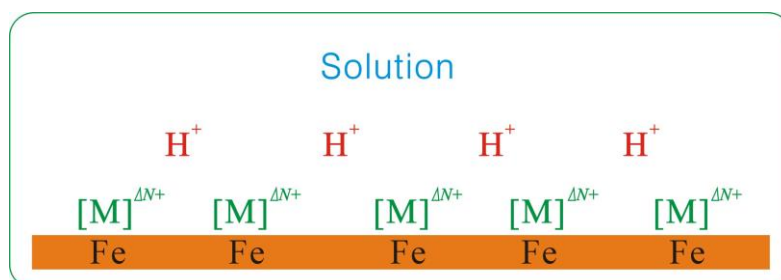

Figure 5. Illustration of the corrosion-inhibition mechanism in HCl solution.
  *$[M]^{\Delta N+}$: Cations formed by corrosion inhibitors

3.4 Prediction of efficiency of corrosion inhibition by new inhibitors

Table 4. Structures of some novel corrosion inhibitors

Inhibitor	Molecular Structure	Inhibitor	Molecular Structure
M4		M8	
M5		M9	
M6		M10	
M7			

The results of this theoretical study were then used to identify the structures of some analogous inhibitors with improved corrosion performance. The core structures of these inhibitors was maintained, with their R2 fragments being replaced by a range of other groups to afford a small series of structurally related compounds (Table 4, M4~M10). Quantum chemical parameters were then carried out on these virtual compounds using DFT/6-31+G(d) calculations, with their *IE* values calculated using formula (3), (4), (6) and (8).

Table 5. Quantum chemical parameters and prediction of *IE* for novel corrosion inhibitors

Inhibitor	E_{HOMO} /eV	E_{LUMO} /eV	ΔE /eV	η	σ	Prediction of inhibition efficiency [a]				Average *IE*%
						Formula(3)	Formula(4)	Formula(6)	Formula(8)	
M4	6.346	1.556	4.790	2.395	0.418	78.28	80.09	79.90	79.63	79.47
M5	6.455	1.519	4.937	2.468	0.405	65.35	67.21	67.01	67.19	66.69
M6	6.337	1.429	4.908	2.454	0.407	69.22	69.70	69.50	69.54	69.49
M7	6.448	1.300	5.147	2.574	0.389	49.12	48.72	48.51	50.58	49.23
M8	6.416	1.411	5.005	2.502	0.400	60.61	61.22	61.02	61.65	61.12
M9	6.421	1.282	5.139	2.570	0.389	50.10	49.42	49.21	51.18	49.97
M10	6.346	1.572	4.775	2.387	0.419	79.45	81.43	81.24	80.96	80.77

[a] formula (3), (4), (6), (8) presented in Table 3.

These theoretical studies revealed that inhibitors M4 and M10 were predicted to exhibit better corrosion inhibitor performance (*IE*% close to 80%) than the parent imines. The three -OH groups of M4 were predicted to be capable of donating more electron density to the metal surface, whilst the R2 group (CH$_3$-C$_6$H$_5$-) of M10 introduces a conjugated aryl ring that would potentially increase its adsorption to the metal surface to afford a better corrosion inhibitory effect.

4. CONCLUSIONS

DFT methods based on B3LYP/6-31+G(d) level calculations have been used to investigate three kinds of Schiff base inhibitors enabling the relationship between *IE* and their quantum chemical structure parameters to be identified. Relationships between their corrosion inhibitor efficiencies and these quantum chemical parameters have been determined and the factors affecting *IE* identified using linear regression analysis. Four formulas describing the relationship between structure and performance have been used to establish that corrosion inhibition properties are dependent on the E_{HOMO} & E_{LUMO}, ΔE, global hardness, softness, and ΔN values of the inhibitor. The theoretical data obtained for these corrosion inhibitors in this study correlated well with previously determined experimental results. These theoretical methods were used to predict the performance of some new corrosion inhibitors, which revealed that two analogous imine inhibitors are likely to exhibit improved corrosion inhibitor properties.

References

1. D.Gopi, Sherif E S M, Manivannan V, *Ind. Eng. Chem. Res.*, 53 (2014) 4286.
2. S.A. Abd El-Maksoud, A.S. Fouda, *Mater. Chem. Phys.*, 93 (2005) 84.
3. G. Gece, *Corros. Sci.*, 50 (2008) 2981.
4. G. Gece, S. Bilgiç, *Corros. Sci.*, 51 (2009) 1876.
5. K. Kalaiselvi, T. Brindha, J. Mallika, *Open J. Met.*, 4 (2014) 73.
6. K.F. Khaled, *Corros. Sci.*, 52 (2010) 2905.
7. J.Hong, Z.P. Kai, L.Yan, *Corros. Sci.*, 50 (2008) 865.
8. N. Soltani, H. Salavati, N. Rasouli, et al, *Chem. Eng. Commun.*, 203 (2016) 840.
9. R.S. Erami, M. Amirnasr, K. Raeissi, et al, *J. Iran. Chem. Soc.*, 12 (2015) 2185.
10. K.R.Ansari, M.A.Quraishi, Ambrish Singh, *J. Ind. Eng. Chem.*, 25 (2015) 89.
11. H. Hamani, T. Douadi, M. Al-Noaimi, et al, *Corros. Sci.*, 88 (2014) 234.
12. A. Aytaç, Ü. Özmen, M. Kabasakaloğlu, *Mater. Chem. Phys.*, 89 (2005) 176.
13. S.H. Kumar, S. Karthikeyan , *Ind. Eng. Chem. Res.*, 52 (2013) 7457.
14. H.M.A. El-Lateef, A.M. Abu-Dief, L.H. Abdel-Rahman, et al, *J. Electroanal. Chem.*, 743 (2015) 120.
15. Canan Küstü，Kaan C. Emregül, Orhan Atakol, *Corros. Sci.*, 49 (2007)2800.
16. S.K. Chen, B. He, *Int. J. Electrochem. Sci.*, 9 (2014) 5400.
17. J.F. Zhu, S.K. Chen, *Int. J. Electrochem. Sci.*, 7 (2012) 11884.
18. I.Ahamad, R. Prasad, M.A. Quraishi, *Mater. Chem. Phys.*, 124 (2010) 1155.
19. HHA Rahman, AHE Moustafa, MK Awad, *Int. J. Electrochem. Sci.*, 7 (2012) 1266.
20. Ayman M Atta, Gamal A El-Mahdy, Adel A. Al-Azhary, *Int. J. Electrochem. Sci.*, 8 (2013) 1295.
21. A.Zarrouk1, H. Zarrok, R. Salghi, et al, *Int. J. Electrochem. Sci.*, 7 (2012) 6353.
22. I. Danaee, O. Ghasemi, G.R. Rashed, et al, *J. Mol. Struct.*, 1035 (2013) 247.
23. W. Kohn, L. J. Sham, *Phys. Rev.*, 140 (1965) A1133.
24. Y. Sasikumar, A.S. Adekunle, L.O. Olasunkanmi, *J. Mol. Liq.*, 211 (2015) 105.
25. T.W. Quadri, L.O. Olasunkanmi, O.E. Fayemi, *ACS Omega.*, 2(2017) 8421.
26. A. V. Marenich, C. J. Cramer, D. G. Truhlar, *J. Phys. Chem. B.*, 113 (2009) 6378.
27. M. J. Frisch, G .W. Trucks, H. B. Schlegel, Gaussian, revision B 09 Pittsburgh, Pa: Gaussian Inc, 2009.
28. V.S. Sastri, J.R. Perumareddi, *Corros. Sci.*, 53 (1997) 617.

29. R.G. Pearson, *Inorg.Chem.*, 316. 27 (1988) 734.
30. I. Lukovits, E. Kalman, F. Zucchi*, Corros*., 57 (2001) 3.
31. S. Martinez, *Mater. Chem. Phys*., 77 (2003) 97.
32. K. Fukui, Theory of Orientation and Stereoselection, Springer-Verlag, New York, 1975.
33. N.O. Obi-Egbedi, I.B. Obot, M.I. El-Khaiary, S.A. Umoren and E.E. Ebenso, *Int. J. Electrochem. Sci.*, 6 (2011) 5649.